# Gibberellin Acts Positively Then Negatively to Control Onset of Flower Formation in *Arabidopsis*

Nobutoshi Yamaguchi *et al.*

*Science* **344**, 638 (2014);
DOI: 10.1126/science.1250498

of VRAC, a notion buttressed by the homology of LRRC8 proteins to pannexins. Because cotransfection of LRRC8 isoforms did not significantly increase $I_{Cl(swell)}$ amplitude over that of the WT, other factors limit VRAC activity; for example, an auxiliary subunit of VRAC or part of the signaling cascade leading to its activation. Indeed, VRAC currents seem to be highly regulated, with amplitudes differing by a factor of only 2 to 3 across cell types (*3*, *30*).

The homology between LRRC8 proteins and pannexins suggested that LRRC8 proteins form hexameric channels (*20*). We confirmed the pannexin-like topology of LRRC8A and propose that VRAC is formed by LRRC8 hexamers of LRRC8A and at least one other family member. In this model, VRAC may contain two to five different LRRC8 isoforms, creating a potentially large variety of VRAC channels with different properties. The variation of $I_{Cl(swell)}$ inactivation kinetics between different tissues and cells (*3*) can be ascribed to different expression ratios of LRRC8 isoforms. LRRC8-dependent $Cl^-$ and taurine fluxes indicated that VRAC is identical to VSOAC (*6*) and fit to a pore formed by LRRC8 hexamers, because hexameric pannexin channels likewise display poor substrate specificity (*28*).

Our results provide the basis to explore the structure-function relationship of VRAC/VSOAC, to clarify the signaling pathway that couples cell volume increase to channel opening, and to investigate the role of the channel in basic cellular processes such as cell division, growth, and migration and in various pathological states. Interestingly, a truncating *LRRC8A* mutation has been described in a patient with agammaglobulinemia (*21*), and *LRRC8C* may have a role in fat metabolism (*31*).

### References and Notes


1. E. K. Hoffmann, I. H. Lambert, S. F. Pedersen, *Physiol. Rev.* **89**, 193–277 (2009).
2. H. Pasantes-Morales, R. A. Lezama, G. Ramos-Mandujano, K. L. Tuz, *Am. J. Med.* **119** (suppl. 1), S4–S11 (2006).
3. B. Nilius *et al.*, *Prog. Biophys. Mol. Biol.* **68**, 69–119 (1997).
4. Y. Okada, K. Sato, T. Numata, *J. Physiol.* **587**, 2141–2149 (2009).
5. Y. Okada, *Am. J. Physiol.* **273**, C755–C789 (1997).
6. P. S. Jackson, K. Strange, *Am. J. Physiol.* **265**, C1489–C1500 (1993).
7. K. Strange, P. S. Jackson, *Kidney Int.* **48**, 994–1003 (1995).
8. I. H. Lambert, E. K. Hoffmann, *J. Membr. Biol.* **142**, 289–298 (1994).
9. D. B. Shennan, *Cell. Physiol. Biochem.* **21**, 15–28 (2008).
10. A. Stutzin *et al.*, *Am. J. Physiol.* **277**, C392–C402 (1999).
11. T. Moser, R. H. Chow, E. Neher, *Pflugers Arch.* **431**, 196–203 (1995).
12. Y. Okada *et al.*, *J. Membr. Biol.* **209**, 21–29 (2006).
13. S. Gründer, A. Thiemann, M. Pusch, T. J. Jentsch, *Nature* **360**, 759–762 (1992).
14. S. C. Stotz, D. E. Clapham, *PLOS ONE* **7**, e46865 (2012).
15. L. T. Chien, H. C. Hartzell, *J. Gen. Physiol.* **132**, 537–546 (2008).
16. R. Fischmeister, H. C. Hartzell, *J. Physiol.* **562**, 477–491 (2005).
17. L. J. Galietta, P. M. Haggie, A. S. Verkman, *FEBS Lett.* **499**, 220–224 (2001).
18. V. Benfenati *et al.*, *Channels* **3**, 323–336 (2009).
19. K. Kubota *et al.*, *FEBS Lett.* **564**, 147–152 (2004).
20. F. Abascal, R. Zardoya, *Bioessays* **34**, 551–560 (2012).
21. A. Sawada *et al.*, *J. Clin. Invest.* **112**, 1707–1713 (2003).
22. L. Cong *et al.*, *Science* **339**, 819–823 (2013).
23. B. Nilius, J. Prenen, U. Wissenbach, M. Bödding, G. Droogmans, *Pflugers Arch.* **443**, 227–233 (2001).
24. C. Y. Hernández-Carballo, J. A. De Santiago-Castillo, T. Rosales-Saavedra, P. Pérez-Cornejo, J. Arreola, *Pflugers Arch.* **460**, 633–644 (2010).
25. G. X. Wang *et al.*, *Am. J. Physiol. Heart Circ. Physiol.* **287**, H533–H544 (2004).
26. J. L. Leaney, S. J. Marsh, D. A. Brown, *J. Physiol.* **501**, 555–564 (1997).
27. G. Smits, A. V. Kajava, *Mol. Immunol.* **41**, 561–562 (2004).
28. S. Penuela, R. Gehi, D. W. Laird, *Biochim. Biophys. Acta* **1828**, 15–22 (2013).
29. S. Maeda *et al.*, *Nature* **458**, 597–602 (2009).
30. B. Nilius *et al.*, *Pflugers Arch.* **428**, 364–371 (1994).
31. T. Hayashi *et al.*, *Biol. Pharm. Bull.* **34**, 1257–1263 (2011).
32. M. Magrane, U. Consortium, *Database (Oxford)* **2011**, bar009 (2011).



**Acknowledgments:** We thank M. Neuenschwander for technical advice concerning the assay; H.-P. Rahn for help with fluorescence-activated cell sorting; A. Brockhoff and W. Meyerhof for use of their Fluorometric Image Plate Reader in a pilot experiment; and J. Liebold, N. Krönke, J. Jedamzick, and S. Kleissle for technical assistance. Supported by the European Research Council Advanced Grant (FP/2007-2013) 294435 "Cytovolion" and the Deutsche Forschungsgemeinschaft (Exc 257 "Neurocure") to T.J.J.


### Supplementary Materials

www.sciencemag.org/content/344/6184/634/suppl/DC1
Materials and Methods
Author Contributions
Figs. S1 to S10
Tables S1 to S4
References (*33*–*38*)


3 March 2014; accepted 2 April 2014
Published online 10 April 2014;
10.1126/science.1252826


# Gibberellin Acts Positively Then Negatively to Control Onset of Flower Formation in *Arabidopsis*


**Nobutoshi Yamaguchi,[1] Cara M. Winter,[1]* Miin-Feng Wu,[1] Yuri Kanno,[2] Ayako Yamaguchi,[1] Mitsunori Seo,[2] Doris Wagner[1]†**



**The switch to reproductive development is biphasic in many plants, a feature important for optimal pollination and yield. We show that dual opposite roles of the phytohormone gibberellin underpin this phenomenon in *Arabidopsis*. Although gibberellin promotes termination of vegetative development, it inhibits flower formation. To overcome this effect, the transcription factor LEAFY induces expression of a gibberellin catabolism gene; consequently, increased LEAFY activity causes reduced gibberellin levels. This allows accumulation of gibberellin-sensitive DELLA proteins. The DELLA proteins are recruited by SQUAMOSA PROMOTER BINDING PROTEIN–LIKE transcription factors to regulatory regions of the floral commitment gene *APETALA1* and promote *APETALA1* up-regulation and floral fate synergistically with LEAFY. The two opposing functions of gibberellin may facilitate evolutionary and environmental modulation of plant inflorescence architecture.**


Synchronization of the developmental transitions that lead to reproductive competence is important for species survival. Plants form new lateral organs iteratively throughout their life from the flanks of the shoot apical meristem (fig. S1) (*1*, *2*). The type of the lateral organ produced depends on the phase of the life cycle. In *Arabidopsis*, rosette leaves are produced during the vegetative phase. During the reproductive phase, an inflorescence forms. Not all lateral organ primordia of the inflorescence are competent to become flowers. Those that are not instead give rise to branches subtended by cauline leaves during the first inflorescence phase (*3*, *4*). The duration of the branch-producing first inflorescence phase determines inflorescence architecture and is critical for optimal seed set.

To gain insight into the regulation of the transition from branch to floral fate in the lateral primordia of the inflorescence, we analyzed public genome-wide binding and expression data and identified genes that are direct targets of the LEAFY (LFY) transcription factor (*5*–*7*) (table S1). LFY promotes flower formation (*8*, *9*). We identified for further study the *EUI-LIKE P450 A1* (*ELA1*) gene (fig. S2), which encodes a cytochrome P450 (*10*). *ELA1* expression was very low in vegetative tissues but increased when flowers formed (fig. S3). On the basis of in situ hybridization and reporter studies, *ELA1* was initially expressed on the abaxial side of incipient flower primordia and later along their entire circumference (Fig. 1A and fig. S3). *ELA1* expression was dependent on the


[1]Department of Biology, University of Pennsylvania, 415 South University Avenue, Philadelphia, PA 19104–6018, USA. [2]RIKEN Center for Sustainable Resource Science, Yokohama, Kanagawa, 230-0045, Japan.

*Present address: Department of Biology, Duke University, Box 90338, Durham, NC 27708, USA.
†Corresponding author. E-mail: wagnerdo@sas.upenn.edu

presence of functional LFY and on the presence of LFY-bound cis elements in the *ELA1* regulatory region (Fig. 1B and fig. S4). To determine whether ELA1 is required for the switch to flower formation in long-day photoperiods, we obtained three mutant alleles (fig. S5). Consistent with its very low expression in vegetative tissues, *ela1* mutants did not alter the duration of the vegetative phase (fig. S5) (*11*). By contrast, loss of *ELA1* function significantly delayed flower formation (Fig. 1C and fig. S5). Thus, ELA1 promotes floral fate in lateral organ primordia of the inflorescence.

*ELA1* functions in catabolism of bioactive gibberellins that are not hydroxylated at the carbon 13 position, such as gibberellin A4 ($GA_4$) (*10*, *11*) (fig. S6). Through up-regulation of *ELA1*, LFY may reduce the levels of $GA_4$ during flower formation. Indeed, analysis of $GA_4$ levels by mass spectrometry after liquid chromatography revealed that this hormone is elevated in *lfy* null mutants and reduced in transgenic plants overexpressing LFY (Fig. 2A and fig. S7). Presence of bioactive gibberellin leads to degradation of DELLA proteins and triggers transcriptional repression of gibberellin biosynthesis genes, including *GIBBERELLIN 20 OXIDASE 2* (*GA20ox2*) (*12*, *13*). Consistent with their elevated levels of $GA_4$, *lfy* inflorescences had reduced levels of the DELLA protein REPRESSOR OF GA1-3 (RGA) and of *GA20ox2* mRNA. In contrast, LFY-overexpressing inflorescences had elevated levels of RGA protein and *GA20ox2* mRNA, relative to wild-type plants (Fig. 2, B and C, and fig. S7). Moreover, removal of ELA1 activity from 35S:LFY plants restored *GA20ox2* mRNA to wild-type levels (fig. S7). In agreement with their altered gibberellin levels, the Gene Ontology term "response to gibberellin stimulus" was significantly enriched (adjusted $P < 0.0005$) among genes differentially expressed in *lfy* mutants or LFY-overexpressing plants (fig. S7). Finally, LFY-overexpressing plants displayed phenotypes characteristic of gibberellin-deficient mutants, such as reduced height and increased chlorophyll content (*14*), that were partly rescued by application of exogenous gibberellin (fig. S7). The data indicate that LFY directs a reduction of gibberellin levels in inflorescences.

In *Arabidopsis*, gibberellin promotes the transition from vegetative development to the first inflorescence phase of reproductive development (*15*–*19*). However, our observations suggest that gibberellin may actually inhibit the transition to flower formation. This result was unexpected because, in general, mutants that delay onset of the first inflorescence phase also delay flower formation, whereas those that accelerate onset of the first inflorescence phase also accelerate flower formation (*20*) (Fig. 3A and fig. S8). We therefore examined the effect of altered gibberellin levels or response on these two transitions. Under long-day conditions, mutants deficient in gibberellin biosynthesis or gibberellin response produced more rosette leaves (delayed onset of the first inflorescence phase) (*19*) but fewer branches and cauline leaves (accelerated flower formation) (Fig. 3B, and fig. S8). Likewise, plants treated with the gibberellin biosynthesis inhibitor paclobutrazol (*21*) had more rosette leaves but fewer branches and cauline leaves (fig. S8). By contrast, plants treated with exogenous gibberellin formed fewer rosette leaves (*15*) and more branches and cauline leaves (Fig. 3C and fig. S8). We then decreased the gibberellin response selectively in lateral organ primordia of the inflorescence, by expressing a negative gibberellin-response regulator (the stabilized DELLA protein rgl1) from the *LFY* promoter. This had no effect on the duration of the vegetative phase but significantly accelerated flower formation (Fig. 3D and fig. S9). These results demonstrate that, whereas gibberellin promotes the transition from vegetative to inflorescence development, it inhibits flower formation.

Reduced gibberellin may increase the competence of lateral organ primordia to adopt a floral fate by enhancing their responsiveness to LFY. To test this hypothesis, we used a constitutively expressed version of LFY fused to the rat glucocorticoid receptor hormone–binding domain (GR), which enables control of LFY activity by dexamethasone (*5*). We also took advantage of the observation that the direct LFY target *APETALA1* (*AP1*) is only expressed in flower primordia (*3*), which makes *AP1* expression a good proxy for floral competence. Simultaneous treatment of plants expressing LFY-GR with dexamethasone and the gibberellin biosynthesis inhibitor paclobutrazol caused increased production of *AP1* in young flower primordia (Fig. 4A and fig. S9), relative to treatment with either paclobutrazol or dexamethasone alone. Via its inhibition of gibberellin biosynthesis, paclobutrazol promotes accumulation of DELLA proteins (*21*, *22*). In agreement with this, dexamethasone treatment of plants expressing both a constitutively expressed DELLA protein fused to GR (RGA-GR) (*23*) and LFY-GR also caused an increase in *AP1* expression (Fig. 4A and fig. S9). The slightly lower expression of *AP1* in RGA-GR LFY-GR plants treated with dexamethasone compared with LFY-GR plants treated with dexamethasone and paclobutrazol may be explained by the ability of paclobutrazol to stabilize multiple DELLA proteins or by degradation of RGA-GR due to the presence of endogenous gibberellin. Although DELLA proteins are best known for their roles in transcriptional repression, they can also activate transcription (*13*, *22*, *24*). Using chromatin immunoprecipitation followed by quantitative polymerase chain reaction (ChIP-qPCR), we found that a tagged version of RGA expressed from its own promoter (*12*) associated with several regulatory regions in the *AP1* locus (Fig. 4B and fig. S9). Moreover, dexamethasone activation of RGA-GR LFY-GR plants in the presence of protein synthesis inhibitor also caused increased *AP1* induction (fig. S9). We conclude that the DELLA

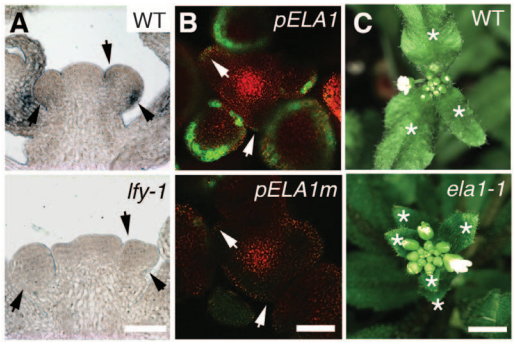


**Fig. 1. *ELA1* is a direct LFY-regulated target and promotes flower formation.** (**A**) *ELA1* in situ hybridization in wild-type (top) and *lfy-1* (bottom) inflorescences. (**B**) GFP reporter expression driven from wild-type (top) or LFY binding site–mutated (bottom) *ELA1* promoter. (A and B) Arrows: young floral primordia. (**C**) Top view of wild-type (top) and *ela1-1* mutant (bottom) inflorescences. The average number of cauline leaves and branches formed was significantly ($P < 10^{-5}$, two-sided Student's *t* test) higher in *ela1-1* (4.6 ± 0.1) than in the wild type (2.8 ± 0.1). Means ± SEM. Asterisks: cauline leaves subtending branches. Scale bars: 50 μm (A) and (B), 5 mm (C).

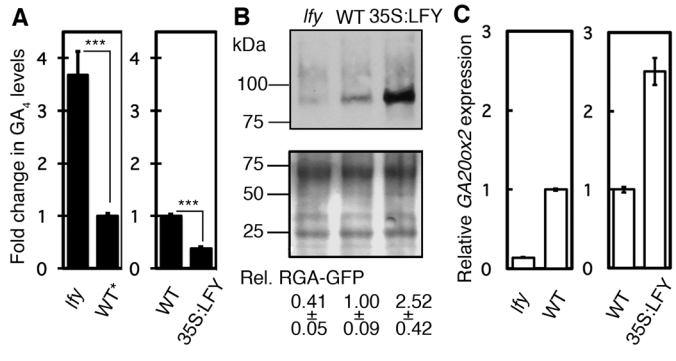


**Fig. 2. LFY causes a reduction of gibberellin levels in the inflorescence.** (**A**) The amount of $GA_4$ in *lfy* null mutant and in 35S:LFY-overexpressing relative to control inflorescences was determined by liquid chromatography–tandem mass spectrometry. ***$P < 10^{-3}$ based on two-sided Student's *t* test. (**B**) (Top) Antibody against GFP in a Western blot of *lfy* null mutant, wild-type (WT), or 35S:LFY inflorescences expressing pRGA:RGA-GFP. (Center) Ponceau S–stained membrane. (Bottom) Band intensity in three biological replicates ($P = 0.007$ for *lfy* versus WT, $P = 0.008$ for 35S:LFY versus WT; two-sided Student's *t* test). (**C**) mRNA abundance of the GA biosynthesis gene *GA20ox2* in *lfy*, wild-type, and 35S:LFY inflorescences. Means ± SEM.

protein RGA potentiates LFY activity and directly promotes the transcription of *AP1*.

DELLA proteins lack DNA binding domains and are thought to be recruited to target loci by sequence-specific transcription factors (*22*). The regulatory regions of the *AP1* locus occupied by RGA were similar to those occupied by a known transcriptional activator of *AP1*, the microRNA miR156 target SQUAMOSA PROMOTER BINDING PROTEIN–LIKE 9 (SPL9) (*25*) (Fig. 4B). SPL9 can physically interact with DELLA proteins (*18*). We therefore next examined the possibility that RGA promotes *AP1* transcription in association with SPL proteins. The *AP1* induction by dexamethasone plus paclobutrazol treatment of LFY-GR was reduced when we simultaneously depleted SPL proteins with an ethanol-inducible version of *MIR156* (*26*) (Fig. 4C), which suggested that SPL proteins contribute to this effect. In agreement with this interpretation, concurrent activation of constitutively expressed SPL9 fused to GR (SPL9-GR) and LFY-GR also led to increased *AP1* induction (Fig. 4C). The synergistic effect of SPL9-GR and LFY-GR on *AP1* induction most likely requires the presence of DELLA proteins, because it was strongly reduced after application of exogenous gibberellin (Fig. 4C). In addition, SPL proteins were necessary for recruitment of RGA to the *AP1* regulatory region both in plants and in yeast one-hybrid assays (Fig. 4D and fig. S9). Finally, increased activity of LFY, SPL9, and DELLA proteins caused flower formation immediately after termination of the vegetative phase (Fig. 4E and fig. S9). We conclude that SPL9 recruits DELLA proteins such as RGA to the *AP1* locus, where they induce *AP1* expression and promote the transformation of lateral primordia into flowers (Fig. 4F).

We reveal a mechanism for sequential coupling of the biphasic transition to reproductive competence in *Arabidopsis thaliana*. This mechanism is based on an increase and a subsequent decrease in hormone levels. Elevated gibberellin promotes termination of the vegetative phase and increases expression of genes encoding transcription factors such as the SPLs and LFY (*16*–*18*, *27*, *28*) (fig. S9). The subsequent reduction in gibberellin levels allows reaccumulation of transcriptional

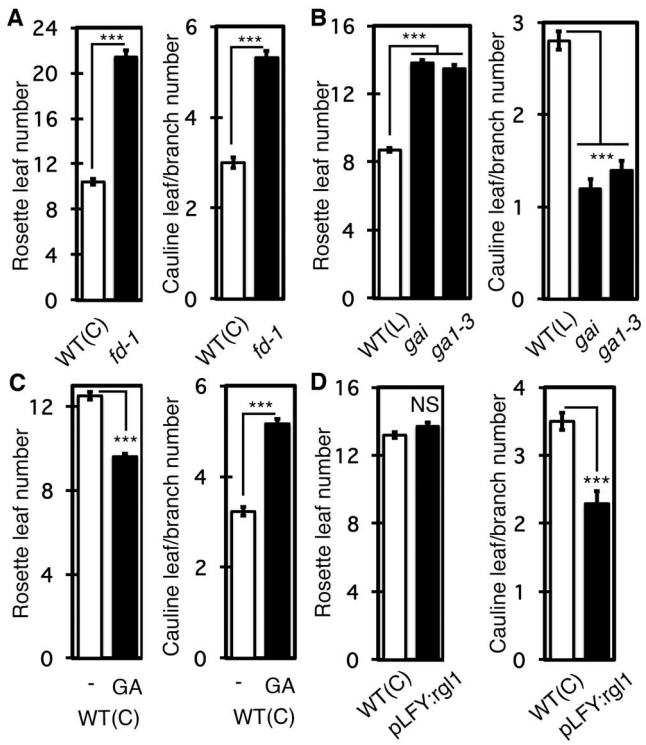


**Fig. 3. Gibberellin inhibits the switch to flower formation.** Duration of the vegetative phase (number of rosette leaves formed) and of the first inflorescence phase (number of cauline leaves and associated branches formed) in long-day photoperiods. White bar (control) and black bar (experimental) genotype or treatment. Means ± SEM. ***$P < 10^{-6}$ based on two-sided Student's *t* test. NS: not significant ($P = 0.25$, two-sided Student's *t* test) (**A**) Typical effect of a mutant [*fd-1* (*20*)] that prolongs both phases. (**B**) Mutants with decreased gibberellin (GA) response (*gai*) or levels (*ga1-3*). (**C**) Treatment with exogenous GA. (**D**) Reduction of the GA response specifically in incipient flower primordia (pLFY:rgl1). Throughout, matched WT genotypes were used [WT (L), wild type in the L*er* accession; WT (C); wild type in the Columbia accession].

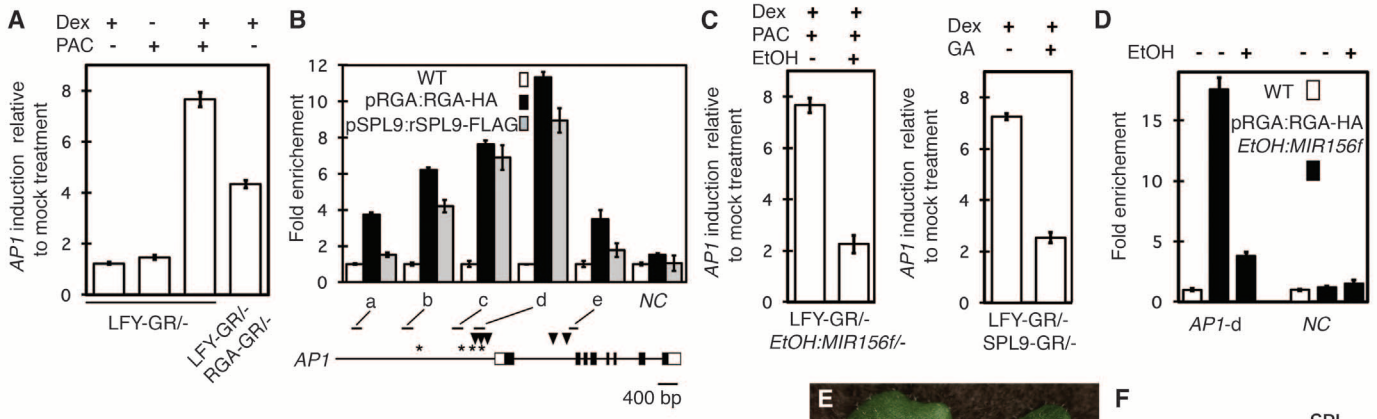


**Fig. 4. Gibberellin-sensitive DELLA transcriptional co-regulators promote floral fate.** (**A**) qRT-PCR determination of *AP1* induction relative to mock treated plants. Treatments: dexamethasone (Dex), gibberellin biosynthesis inhibitor paclobutrazol (PAC). (**B**) ChIP-qPCR of pRGA:RGA-HA and pSPL9:rSPL9-FLAG inflorescences using antibodies against hemagglutinin (HA) and FLAG. WT: ChIP in nontransgenic wild-type plants. NC: negative control locus. (Bottom) *AP1* promoter with PCR fragments amplified. Asterisks, SPL binding motifs; triangles, LFY binding motifs. (**C**) qRT-PCR determination of *AP1* induction relative to mock treated plants. Treatments: Dex, PAC, ethanol vapor induction of ETOH:*MIR156f* (*26*) to deplete miR156-sensitive SPL proteins, or GA to deplete DELLA proteins (*12*). (**D**) pRGA:RGA-HA association with the *AP1* locus "d" region in the presence (-ETOH) or absence (+ETOH) of miR156-sensitive SPL proteins. ChIP controls were as in (B). (A) to (D) Means ± SEM. (**E**) Immediate switch to flower formation in plants with increased LFY (35S:LFY), SPL9 (miR156 resistant pSPL9:rSPL9-FLAG) and DELLA (PAC treatment) levels. The number of cauline leaves formed in 35S:LFY pSPL9:rSPL9-FLAG PAC plants (0.3 ± 0.1) was significantly less ($P < 10^{-16}$, two-sided Student's *t*-test) than that of 35S:LFY plants (2.5 ± 0.2). (**F**) LFY and SPL9/DELLA synergistically induce *AP1*.

co-regulators, the DELLA proteins (*12*), which potentiate the ability of SPL9 (directly) and LFY (indirectly) to induce *AP1* and to trigger the onset of flower formation (fig. S9). LFY initiates the reduction in gibberellin levels—which results in increased DELLA accumulation—at least in part by inducing expression of the gibberellin catabolism enzyme ELA1.

Our findings may help explain the previously paradoxical observation that gibberellin acts positively in the switch to reproductive development in most plants but negatively in some woody plant species, such as grapevine (*29*). In addition, our data make gibberellin a prime candidate for a "branching" factor predicted by mathematical modeling of inflorescence architectures (*30*). Finally, our results suggest that the degree of inflorescence branching, which determines seed yield and, thus, reproductive success, could be adjusted by altering gibberellin accumulation before the inflorescence forms or the rate of gibberellin catabolism thereafter.

### References and Notes


1. T. A. Steeves, I. Sussex, *Pattern in Plant Development* (Cambridge Univ. Press, Cambridge, 1989).
2. R. S. Poethig, *Science* **250**, 923–930 (1990).
3. O. J. Ratcliffe, D. J. Bradley, E. S. Coen, *Development* **126**, 1109–1120 (1999).
4. F. D. Hempel *et al.*, *Development* **124**, 3845–3853 (1997).
5. C. M. Winter *et al.*, *Dev. Cell* **20**, 430–443 (2011).
6. M. Schmid *et al.*, *Nat. Genet.* **37**, 501–506 (2005).
7. M. Schmid *et al.*, *Development* **130**, 6001–6012 (2003).
8. D. Weigel, J. Alvarez, D. R. Smyth, M. F. Yanofsky, E. M. Meyerowitz, *Cell* **69**, 843–859 (1992).
9. D. Weigel, O. Nilsson, *Nature* **377**, 495–500 (1995).
10. Y. Zhang *et al.*, *Plant J.* **67**, 342–353 (2011).
11. T. Nomura *et al.*, *Plant Cell Physiol.* **54**, 1837–1851 (2013).
12. A. Dill, H. S. Jung, T. P. Sun, *Proc. Natl. Acad. Sci. U.S.A.* **98**, 14162–14167 (2001).
13. R. Zentella *et al.*, *Plant Cell* **19**, 3037–3057 (2007).
14. M. Koornneef, J. H. van der Veen, *Theor. Appl. Genet.* **58**, 257–263 (1980).
15. J. Langridge, *Nature* **180**, 36–37 (1957).
16. V. C. Galvão, D. Horrer, F. Küttner, M. Schmid, *Development* **139**, 4072–4082 (2012).
17. A. Porri, S. Torti, M. Romera-Branchat, G. Coupland, *Development* **139**, 2198–2209 (2012).
18. S. Yu *et al.*, *Plant Cell* **24**, 3320–3332 (2012).
19. R. N. Wilson, J. W. Heckman, C. R. Somerville, *Plant Physiol.* **100**, 403–408 (1992).
20. M. Koornneef, C. J. Hanhart, J. H. van der Veen, *Mol. Gen. Genet.* **229**, 57–66 (1991).
21. W. Rademacher, *Annu. Rev. Plant Physiol. Plant Mol. Biol.* **51**, 501–531 (2000).
22. J. M. Davière, P. Achard, *Development* **140**, 1147–1151 (2013).
23. X. Hou, L. Y. Lee, K. Xia, Y. Yan, H. Yu, *Dev. Cell* **19**, 884–894 (2010).
24. K. Hirano *et al.*, *Plant J.* **71**, 443–453 (2012).
25. J. W. Wang, B. Czech, D. Weigel, *Cell* **138**, 738–749 (2009).
26. N. Yu *et al.*, *Plant Cell* **22**, 2322–2335 (2010).
27. M. A. Blázquez, D. Weigel, *Nature* **404**, 889–892 (2000).
28. S. Eriksson, H. Böhlenius, T. Moritz, O. Nilsson, *Plant Cell* **18**, 2172–2181 (2006).
29. P. K. Boss, M. R. Thomas, *Nature* **416**, 847–850 (2002).
30. P. Prusinkiewicz, Y. Erasmus, B. Lane, L. D. Harder, E. Coen, *Science* **316**, 1452–1456 (2007).



**Acknowledgments:** We are grateful to Wagner laboratory members and K. Gallagher, R. S. Poethig, and J. D. Wagner for critical comments. We thank R. Austin for the LFY binding motif functional depth analyses, T. Sun for pRGA:RGA-GFP and GA pathway mutant seeds, X. Chen for *35S:AlcR pAlcA:MIR156f* and pRGA:RGA-HA seeds, M. Schmid for RGL1 and rgl1delta17 constructs, S. Poethig for pSPL9:rSPL9-FLAG and 35S:SPL9-GR seeds, H. Yu for *ga1-3 rgl2-1 rga-2* 35S:RGA-GR seeds, G. Angenent for pAP1:AP1-GFP seeds, and the *Arabidopsis* Biological Resource Center for insertion mutant seeds and the F6A4 bacterial artificial chromosome clone. This work was supported by NSF grants IOS 0849298 and 1257111 to D.W. and training grant T32-HD007516 (Developmental Biology) support to C.M.W.


**Supplementary Materials**

www.sciencemag.org/content/344/6184/638/suppl/DC1
Materials and Methods
Figs. S1 to S9
Tables S1 and S2
References (*31*–*65*)


7 January 2014; accepted 2 April 2014
10.1126/science.1250498


# Cancer Immunotherapy Based on Mutation-Specific CD4+ T Cells in a Patient with Epithelial Cancer


**Eric Tran,[1] Simon Turcotte,[1]* Alena Gros,[1] Paul F. Robbins,[1] Yong-Chen Lu,[1] Mark E. Dudley,[1]† John R. Wunderlich,[1] Robert P. Somerville,[1] Katherine Hogan,[1] Christian S. Hinrichs,[1] Maria R. Parkhurst,[1] James C. Yang,[1] Steven A. Rosenberg[1]‡**



Limited evidence exists that humans mount a mutation-specific T cell response to epithelial cancers. We used a whole-exomic-sequencing-based approach to demonstrate that tumor-infiltrating lymphocytes (TIL) from a patient with metastatic cholangiocarcinoma contained CD4+ T helper 1 ($T_H1$) cells recognizing a mutation in erbb2 interacting protein (ERBB2IP) expressed by the cancer. After adoptive transfer of TIL containing about 25% mutation-specific polyfunctional $T_H1$ cells, the patient achieved a decrease in target lesions with prolonged stabilization of disease. Upon disease progression, the patient was retreated with a >95% pure population of mutation-reactive $T_H1$ cells and again experienced tumor regression. These results provide evidence that a CD4+ T cell response against a mutated antigen can be harnessed to mediate regression of a metastatic epithelial cancer.


The human immune system has evolved to recognize and eliminate cells expressing foreign, nonself antigens. All malignant tumors harbor nonsynonymous mutations or other genetic alterations (*1*), some of which may generate neo-"nonself" epitopes that could potentially trigger an antitumor T cell response. Indeed, mutation-reactive T cells can frequently be found infiltrating human melanomas (*2*) and likely play a critical role in the clinical efficacy of adoptive cell therapy (ACT) and other immunotherapies in melanoma (*3*–*7*). However, limited evidence exists demonstrating that the human immune system can mount an endogenous, mutation-specific T cell response against epithelial cancers that comprise over 80% of all human malignancies (*8*-*11*), and it is unclear whether this response can be harnessed to develop effective personalized cancer immunotherapies (*12*). Moreover, epithelial cancers often contain fewer mutations than melanoma (*1*), which may decrease the probability of eliciting a mutation-specific T cell response. We thus first set out to determine whether tumor-infiltrating lymphocytes (TIL) recognizing patient-specific mutations can be identified in patients with metastatic gastrointestinal (GI) cancers.

To this end, a 43-year-old woman with widely metastatic cholangiocarcinoma (patient 3737, table S1) who progressed through multiple chemotherapy regimens was enrolled in a TIL-based ACT protocol for patients with GI cancers (NCT01174121) (*13*). Lung metastases were resected and used as a source for whole-exomic sequencing and generation of T cells for treatment. Whole-exomic sequencing revealed 26 nonsynonymous mutations (table S2). To test whether the patient's TIL recognized any of these mutations, we used a minigene approach. Briefly, for each mutation we designed a minigene construct that encoded for the mutated amino acid flanked on each side by 12 amino acids from the endogenous protein (fig. S1). Multiple minigenes were synthesized in tandem to generate tandem minigene (TMG) constructs (fig. S1 and table S3), which were then used as templates for the generation of in vitro transcribed (IVT) RNA (*13*). Each of these IVT TMG RNAs was then


[1]Surgery Branch, National Cancer Institute (NCI), National Institutes of Health, Bethesda, MD 20892, USA.

*Present address: Department of Surgery, Université de Montréal, and Institut du Cancer de Montréal, Centre de Recherche du Centre Hospitalier de l'Université de Montréal, Montréal, QC H2X0A9, Canada.

†Present address: Cell and Gene Therapies, Novartis Institutes for BioMedical Research Incorporated, Cambridge, MA 02139, USA.

‡Corresponding author. E-mail: sar@nih.gov